Supporting Information

Adam E. Thomas[1], Hayley S. Glicker[1], Alex B. Guenther[2], Roger Seco[3], Oscar Vega Bustillos[4], Julio Tota[5], Rodrigo A. F. Souza[6], and James N. Smith[1]

[1]Department of Chemistry, University of California, Irvine, USA
[2]Department of Earth System Science, University of California, Irvine
[3]Institute of Environmental Assessment and Water Research (IDAEA-CSIC), Barcelona, Catalonia, Spain
[4]Instituto de Pesquisas Energéticas e Nucleares, Cidade Universitaria, São Paulo, Brazil
[5]Universidade Federal do Oeste do Pará, Santarém, Brazil
[6]Escola Superior de Tecnologia, Universidade do Estado do Amazonas, Manaus, Brazil

Correspondence: James N. Smith (jimsmith@uci.edu)

1 Information on α-pinene ozonolysis experiments

α-Pinene ozonolysis particles were generated in a continuous flow experiment in an 8 L glass flow tube and collected with the sequential spot sampler (Aerosol Devices Inc.) over a 24 h period. Ozone was introduced by passing 2 L/min of clean "zero" air (model 747-30, Aadco Instruments) over an Hg UV lamp (model 90-0004-04, UVP, LLC). α-Pinene was introduced by taking 0.09 L/min from a gas cylinder containing 16.7 ppm of precursor. Reagent flows into the tube were mixed and diluted with zero air to achieve a total inlet flow of 4.6 L/min and concentrations of >1 ppm ozone, as monitored by an ozone analyzer (model 106L, 2B Technology), and an estimated 330 ppb α-pinene. Particles were collected at 3 L/min in a single sample well and extracted in 70 μL of a 1:1 mix of acetonitrile HPLC grade, Sigma Aldrich) and water (HPLC grade, Sigma Aldrich) for 30 min. Extract was analyzed with no further preparation using the same LC/MS method described in the main text.
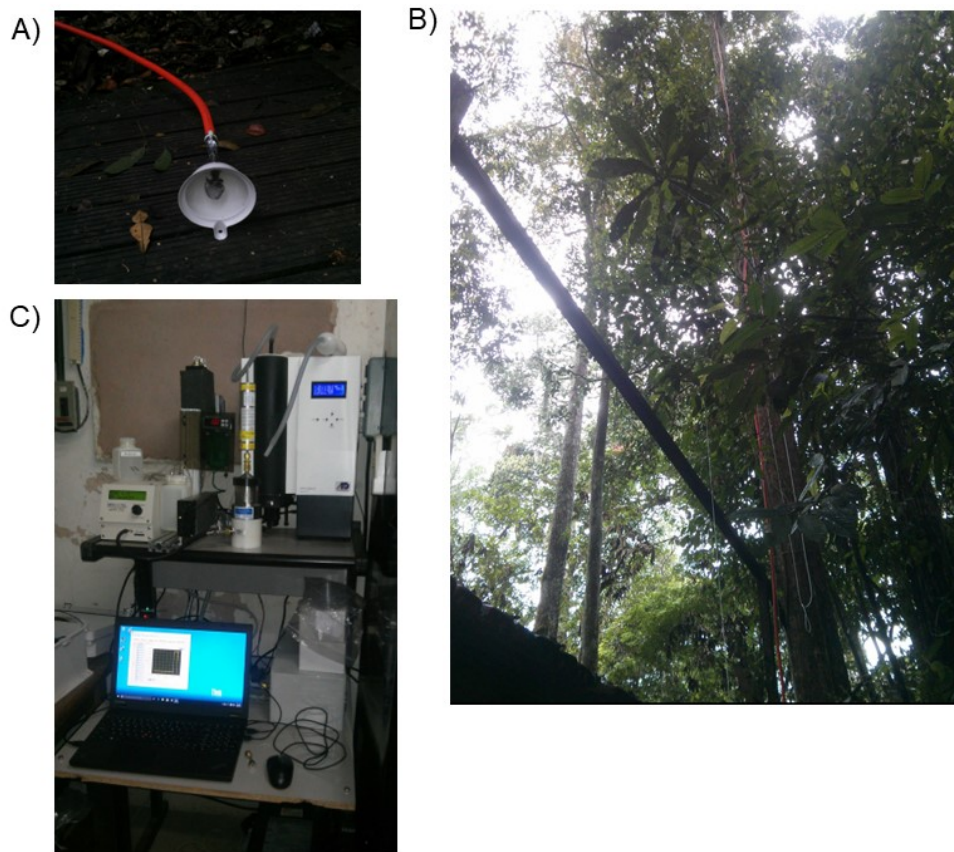
Figure S1. (A) Sample inlet head located near the tree canopy top at the KM67 measurement site (2.857° S, 54.959° W). (B) 30 m sampling line connecting inlet head to instrument housing below. (C) Sequential spot sampler with nano-DMA (TSI, model 3085) connected upstream.
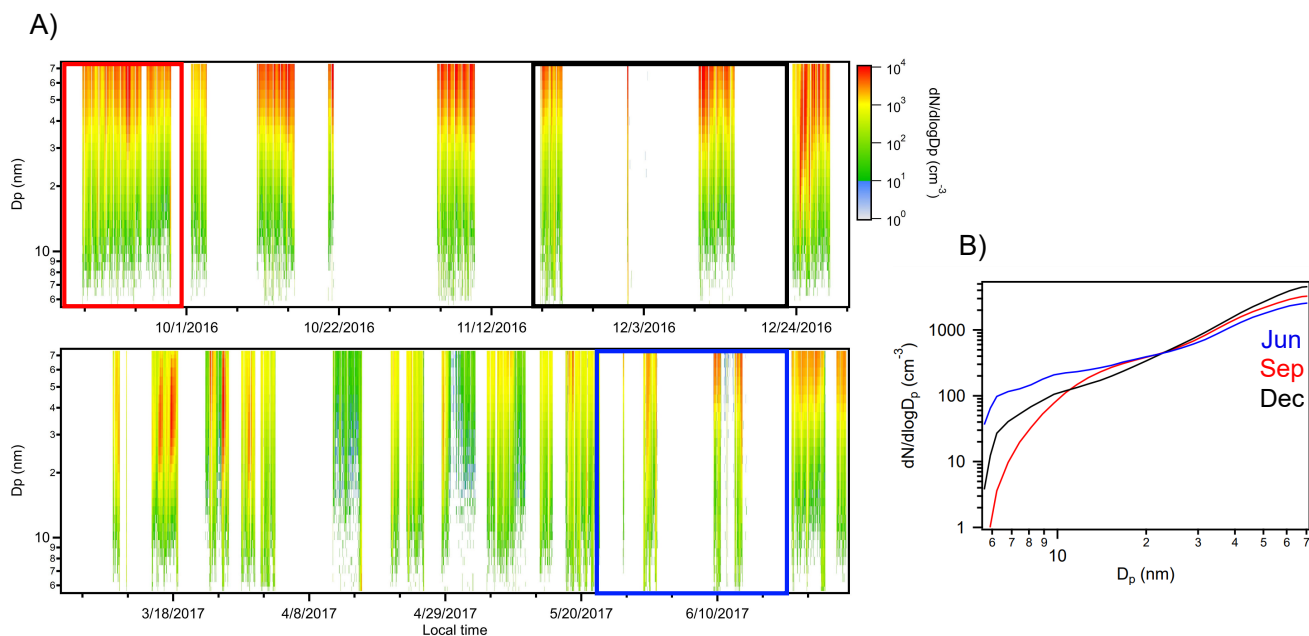
Figure S2. (A) Particle number-size distribution measurements (scanning particles with diameters 5 - 70 nm) taken at the Km67 measurement site from September 2016 through June 2017. The top panel roughly corresponds to the late dry season (September - December) while the bottom corresponds to the wet season (January - June) and wet-dry transition (June-July). White bars indicate when instrument was not working properly. (B)Average particle number-size distributions for the three seasonal periods when particles were sampled. Sep: 10 - 30 September 2016 (red), Dec: 18 November - 23 December 2016 (black), Jun: 22 May - 21 June 2017 (blue).
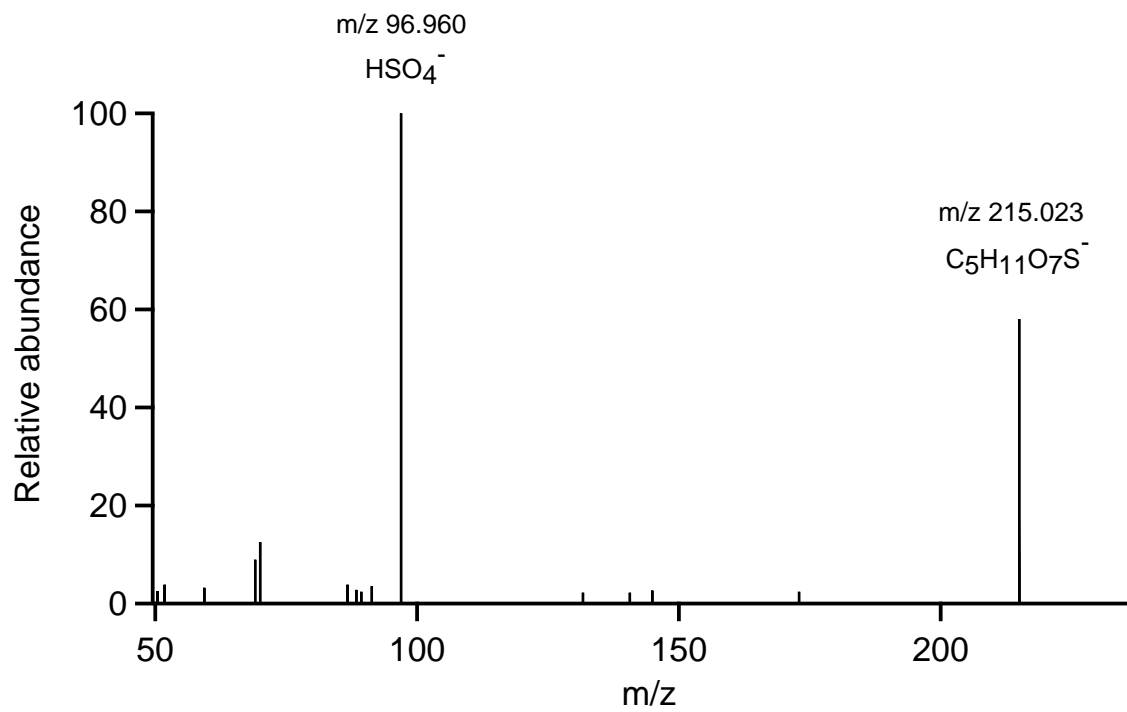
Figure S3. Representative MS2 fragmentation spectrum with major peaks assigned for *m/z* 215.023 as observed in SEP.
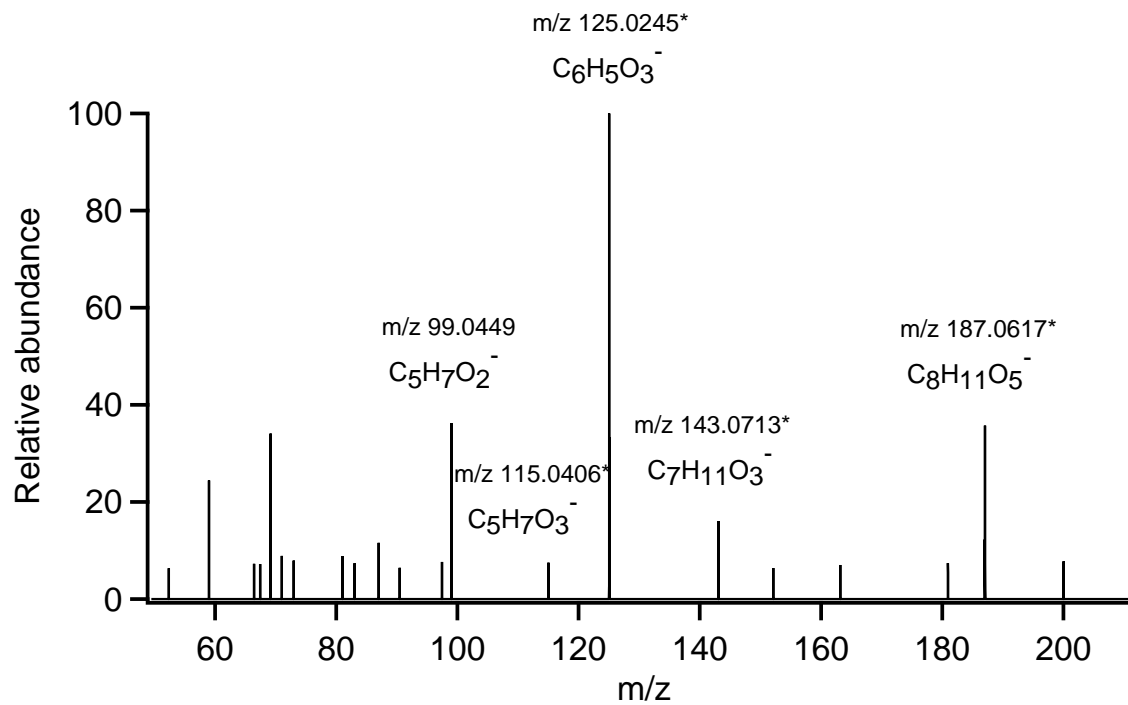
Figure S4. Representative MS2 fragmentation spectrum with major peaks assigned for *m/z* 187.061 as observed in SEP. Starred ions are fragments with same unit masses reported by Kahnt et al. (2014) for hydroxyterpenylic acid isomers.
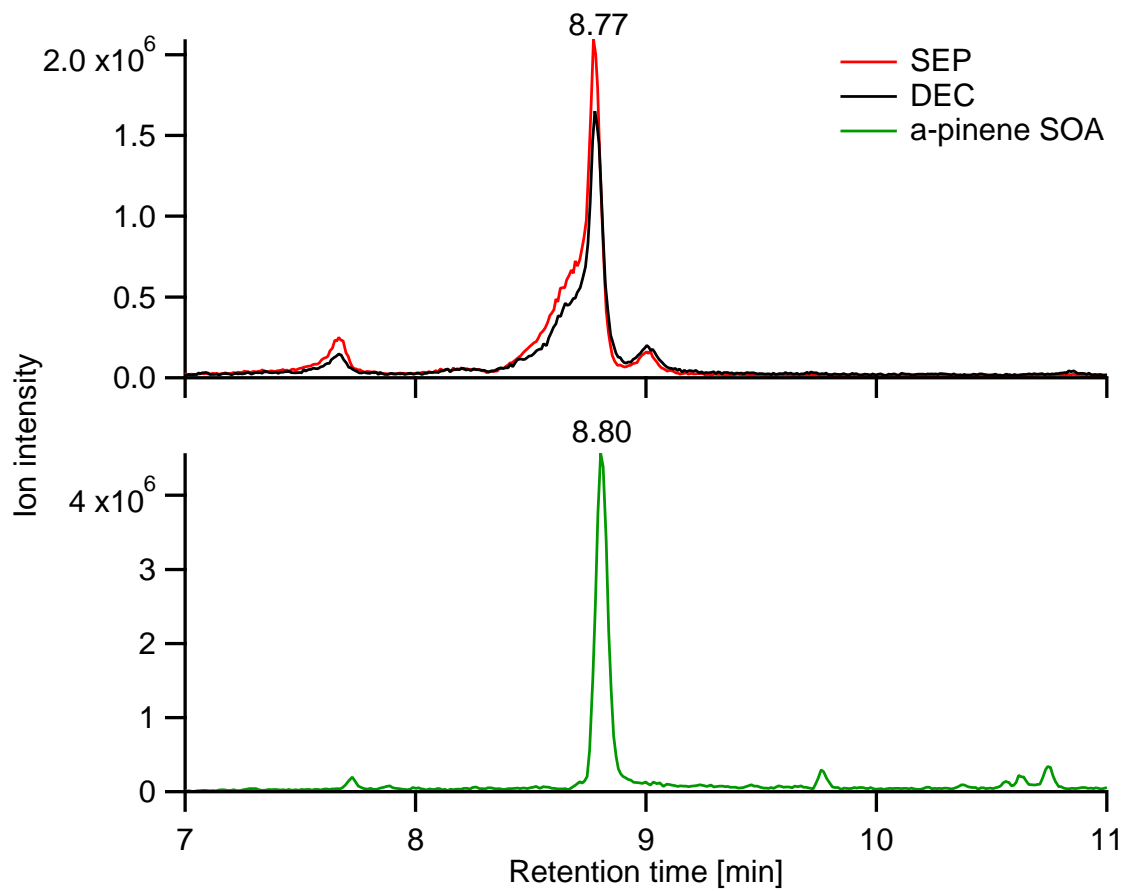
Figure S5. Extracted ion current chromatograms for *m/z* 187.098 (assigned a neutral formula of $C_9H_{16}O_4$) as observed in SEP (red), DEC (black) and from the α-pinene ozonolysis experiments (a-pinene SOA) (green).
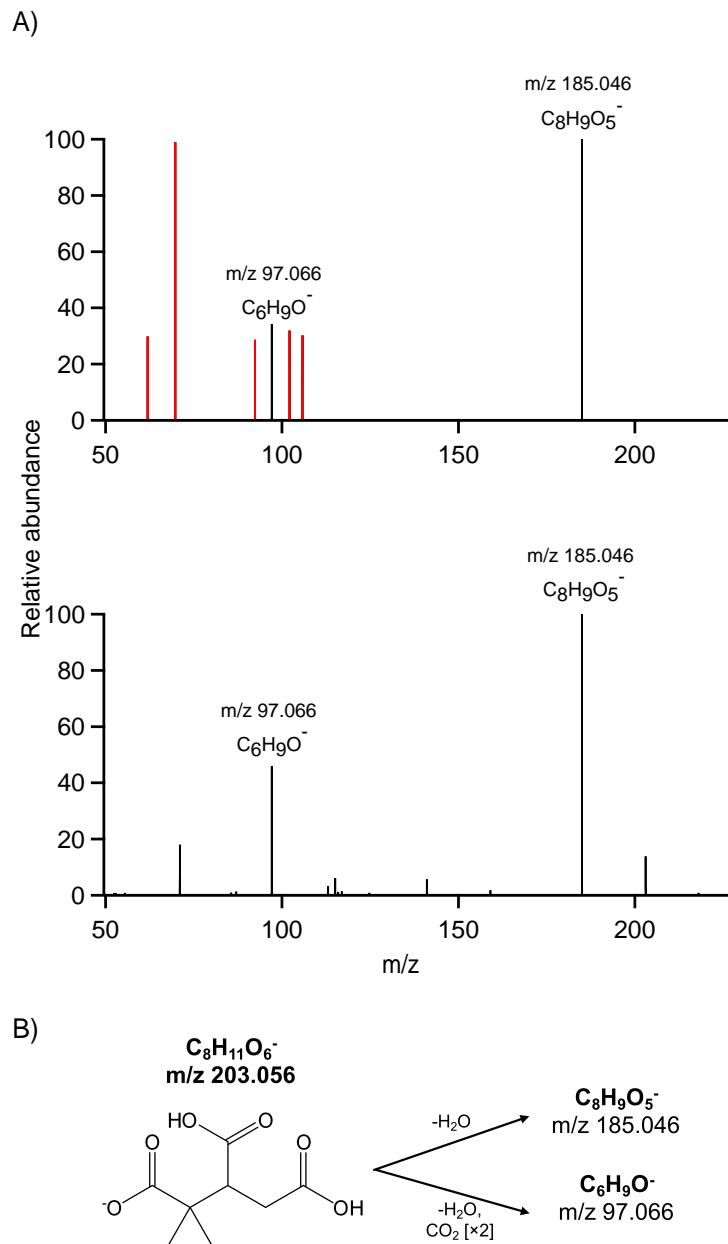
Figure S6. (A) Representative MS2 fragmentation spectrum with major peaks assigned for *m/z* 203.056 in SEP (top) and from the α-pinene ozonolysis experiments (bottom). Peaks highlighted in red for SEP are suspected contamination/interference as they could not be assigned CHO formulae. (B) Proposed fragmentation mechanism based on Szmigielski et al. (2007).
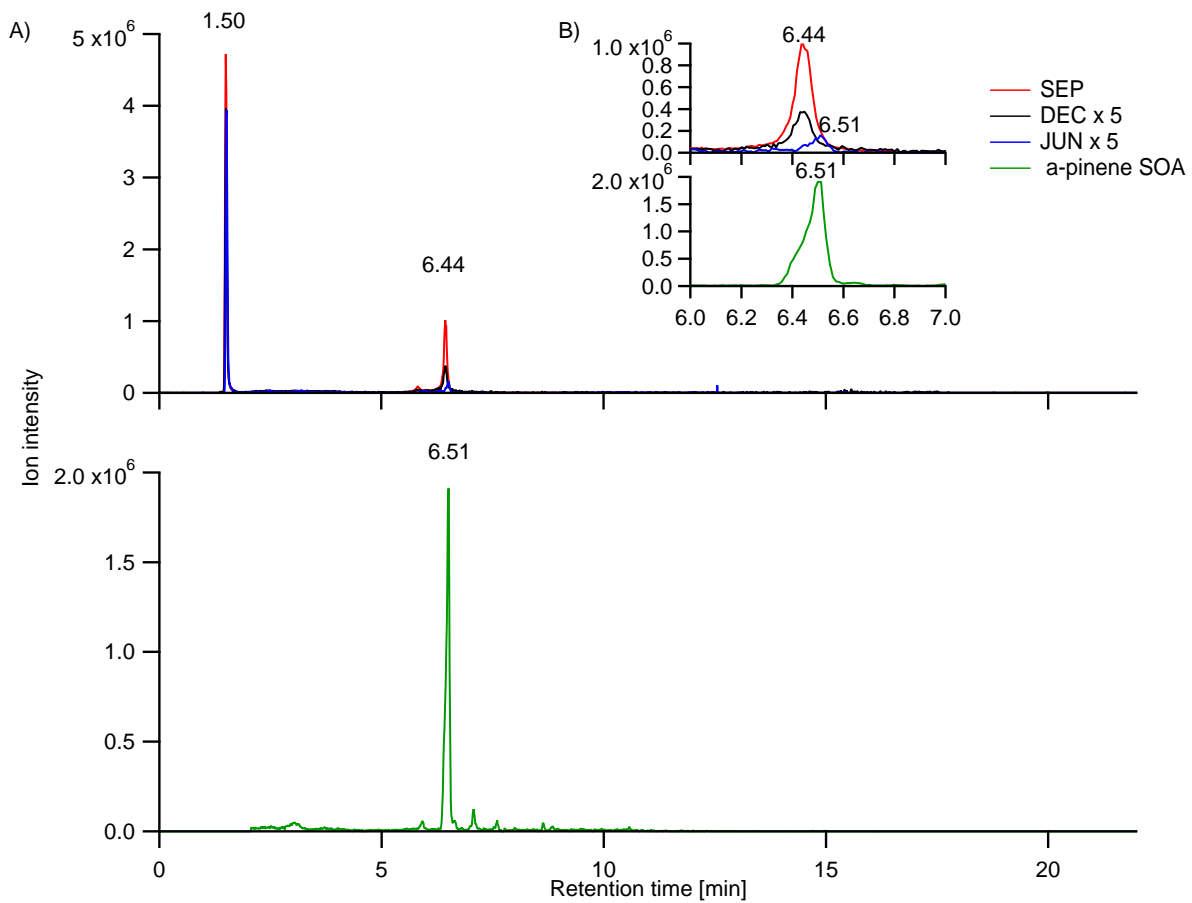
Figure S7. Extracted ion current chromatograms for m/z 203.056 (assigned a neutral formula of $C_6H_{16}O_4$) as observed in SEP (red), DEC (black) and from the α-pinene ozonolysis experiments (a-pinene SOA) (green).
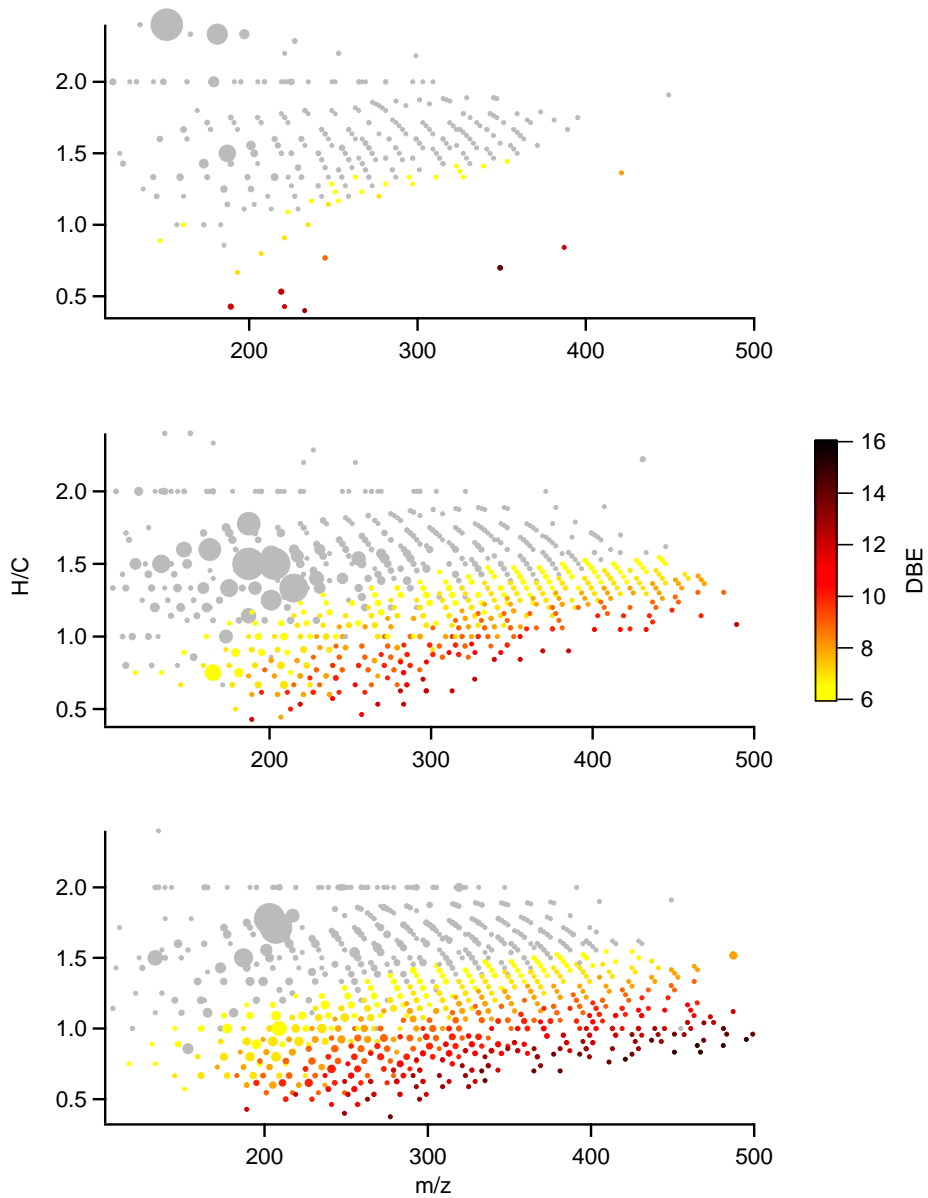
Figure S8. Distribution of double bond equivalents (DBE) for CHO-containing molecules observed in each seasonal period. Marker size indicates ion relative abundance.
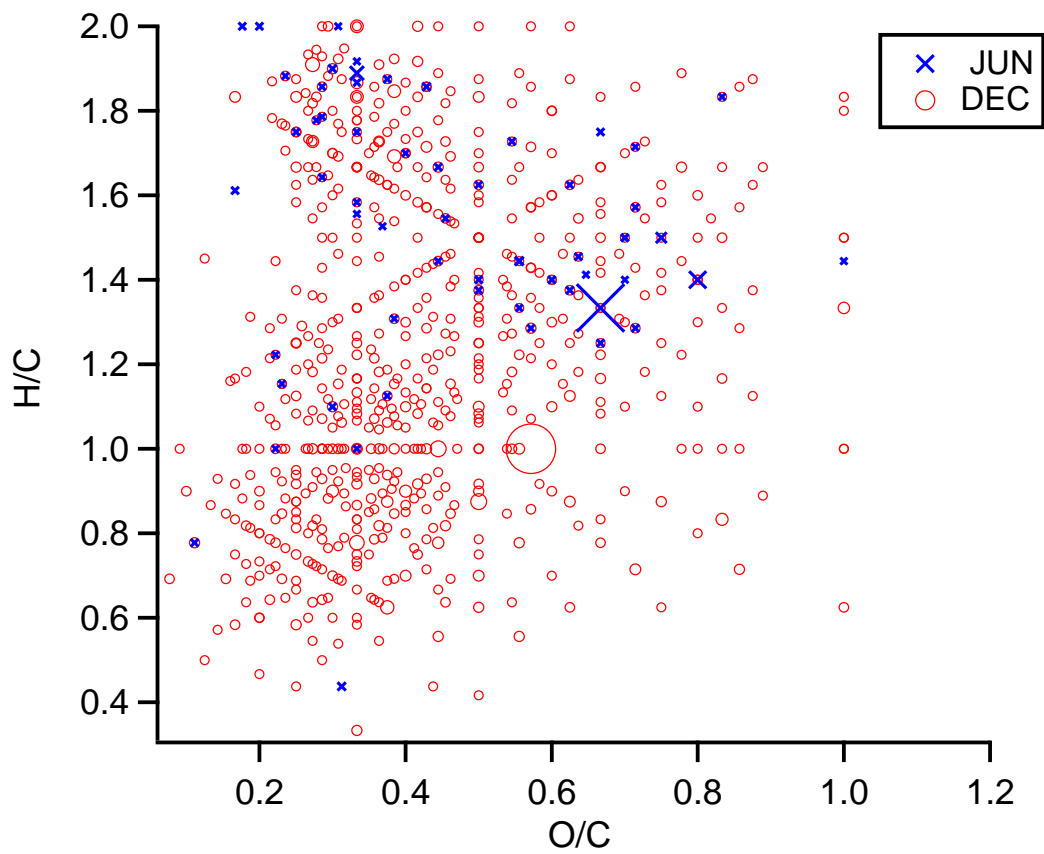
Figure S9. Van Krevelen diagram of the CHON molecules observed in JUN (blue circles) and DEC (red squares). Marker size indicates relative ion abundance.
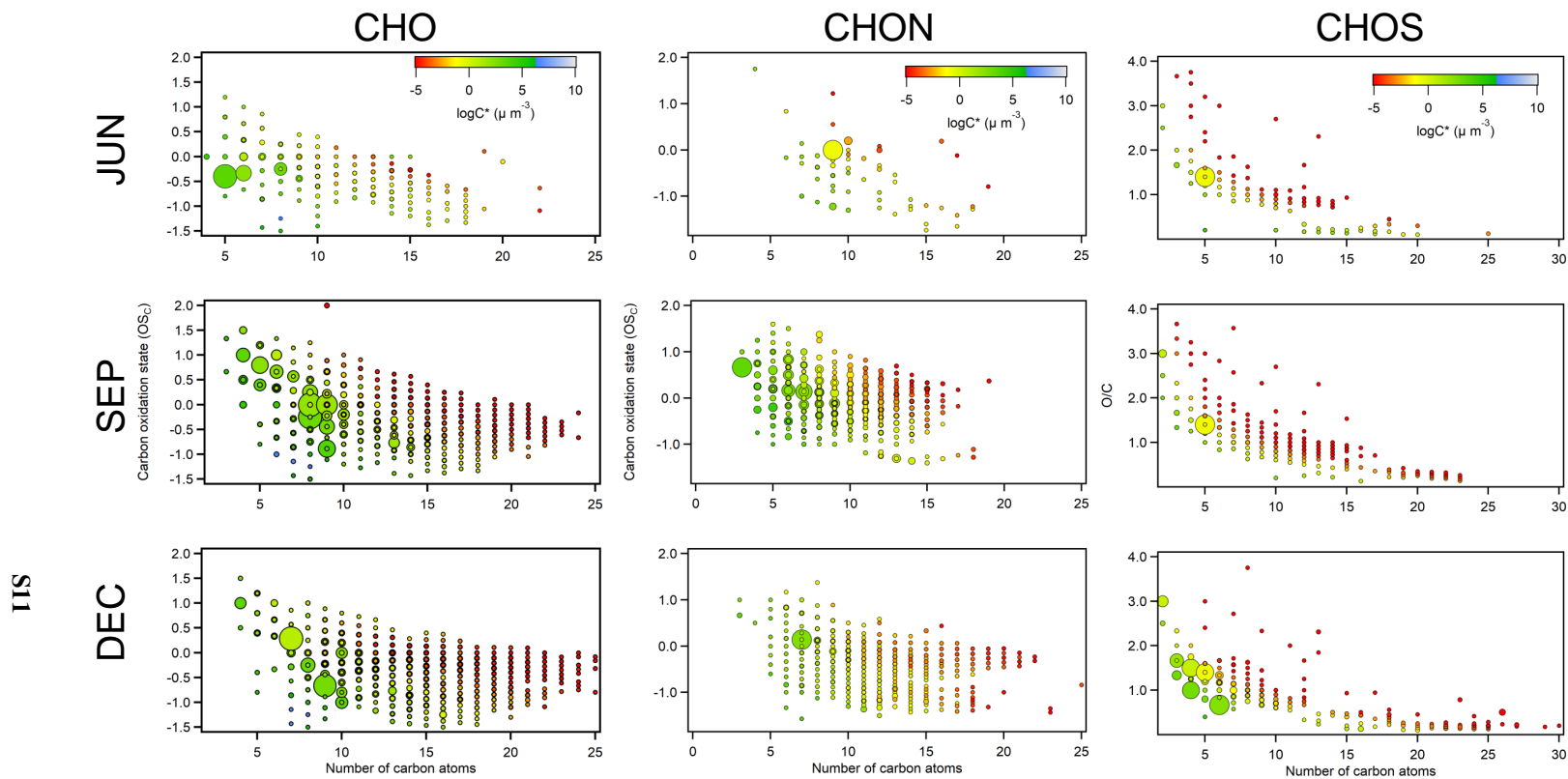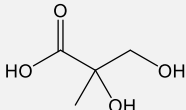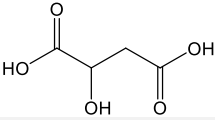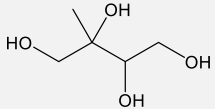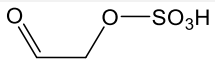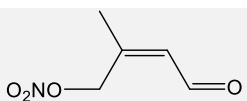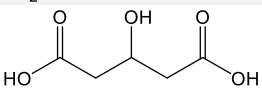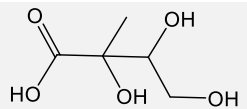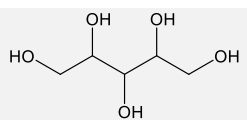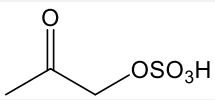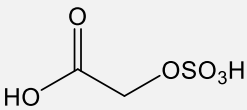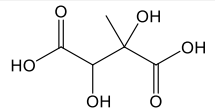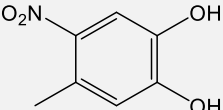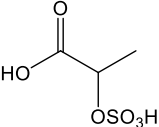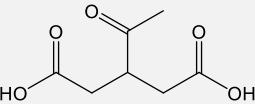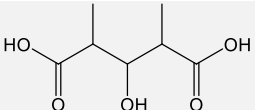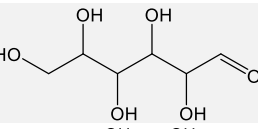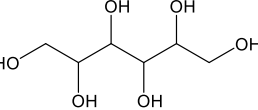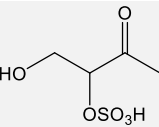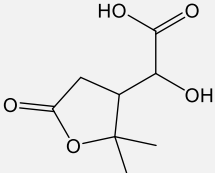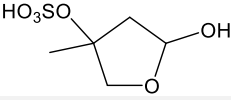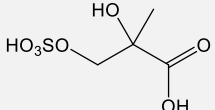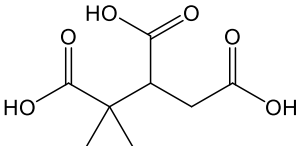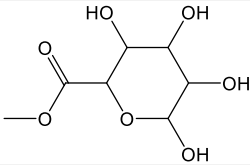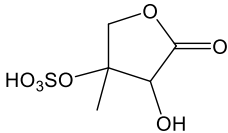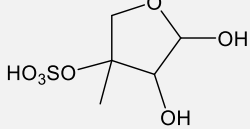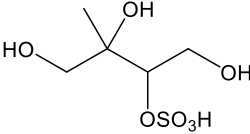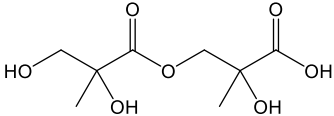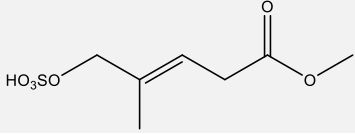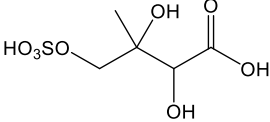
Figure S10. Molecular volatility distributions (logC*, color axis) depicted as a function of carbon oxidation state and carbon number for the three main compound classes observed in each seasonal period. The warmer the color the lower the saturation concentration (lower volatility). CHOS molecules are depicted against O/C ratio instead of carbon oxidation state to avoid functionality assumptions due to the likely strong presence of organosulfate species.
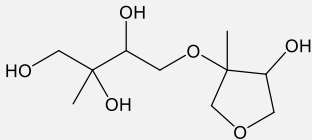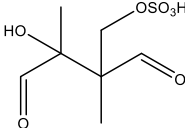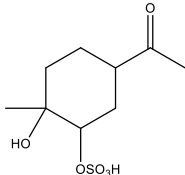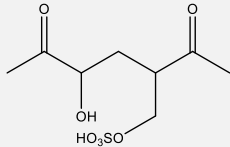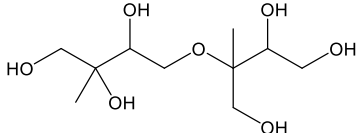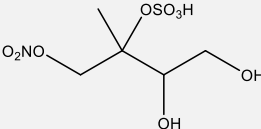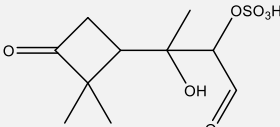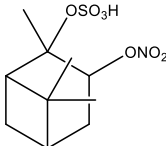
3 Supporting Tables
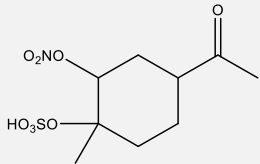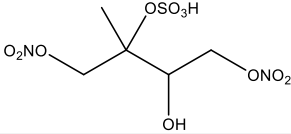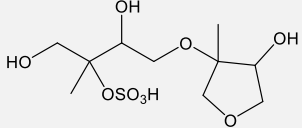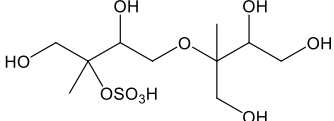
Table S1. List of observed compounds discussed in main text with suggested chemical structures and potential sources.

Theoretical *m/z* ([M-H]⁻)	Molecular Formula ([M-H]⁻)	Suggested Parent Structure	Sample(s) Observed*	Mass Error(s) (ppm)	Potential Source(s)**
119.0350	$C_4H_7O_4^-$		S J	0.1 0.7	Isoprene oxidation[1]
133.0142	$C_4H_5O_5^-$		S D	-0.1 -0.5	Biogenic VOC photooxidation[2–4]
135.0663	$C_5H_{11}O_4^-$		S D J	-0.1 -1.4 -0.7	Isoprene oxidation[1]
138.9707	$C_2H_3O_5S^-$		S D J	0.1 -0.5 -0.4	Isoprene organosulfate chemistry[5]
144.0302	$C_5H_6O_4N^-$		S D	-0.3 -0.7	NO₃ oxidation of isoprene[6]
147.0299	$C_5H_7O_5^-$		S D J	-0.7 -0.4 -0.6	Monoterpene oxidation[7]
149.0455	$C_5H_9O_5^-$		J	0.3	Isoprene oxidation[4,8]
151.0071	$C_4H_7O_4S^-$	?	D	0.3	PAH oxidation in presence of SO_2[9]
151.0612	$C_5H_{11}O_5^-$		S J	0.1 0.4	Biological spores[10]
152.9863	$C_3H_5O_5S^-$		S D J	-0.2 0.1 0.2	Isoprene organosulfate chemistry[5]
154.9656	$C_2H_3O_6S^-$		S D J	-0.7 -0.5 -0.1	Isoprene organosulfate chemistry[1]
163.0248	$C_5H_7O_6^-$		S D J	-0.6 -1.1 -0.5	Isoprene oxidation[1]

m/z	Formula	Structure	Ion	Value	Source
168.0302	$C_7H_6O_4N^-$		S	0.1	Biomass
			D	-1.0	burning[11]
168.9812	$C_3H_5O_6S^-$		S	0.2	Isoprene organosulfate
			J	-0.2	chemistry[1]
173.0455	$C_7H_9O_5^-$		D	0.3	Monoterpene
			J	-0.2	oxidation[12]
173.0819	$C_8H_{13}O_4^-$	?	S	-0.3	Monoterpene
			J		oxidation[13]
175.0612	$C_7H_{11}O_5^-$		S	-0.1	Monoterpene
			D	0.1	oxidation[12]
			J	-0.3	
179.0384	$C_6H_{11}O_4S^-$	?	D	-0.9	PAH oxidation in presence of SO_2[9]
179.0561	$C_6H_{11}O_6^-$		J	-0.2	Primary biogenic emissions[10,14]
181.0718	$C_6H_{13}O_6^-$		J	0.3	Biological spores[10]
182.9969	$C_4H_7O_6S^-$		S	-0.8	Isoprene
			D	-0.6	organosulfate
			J	-0.6	chemistry[1]
184.9761	$C_3H_5O_7S^-$	?	S	0.1	Isoprene
			D	0.1	organosulfate chemistry[15]
187.0612	$C_8H_{11}O_5^-$		S	-0.3	
			D	-0.1	Monoterpene
			J	0.1	oxidation[16]
197.0125	$C_5H_9O_6S^-$		S	0.3	Isoprene
			D	0.0	organosulfate
			J	-0.6	chemistry[17]
198.9918	$C_4H_7O_7S^-$		D	0.3	Isoprene
			J	-0.6	organosulfate chemistry[1]

m/z	Formula	Structure		Value	Source
203.0561	$C_8H_{11}O_6^-$		S	-1.2	Monoterpene oxidation[18]
			D	-1.0	
			J	-0.2	
203.0925	$C_9H_{15}O_5^-$	?	D	-0.9	Aromatic oxidation product[19]
207.0510	$C_7H_{11}O_7^-$		S	0.6	Biomass burning[20]
			D	-0.2	
			J	0.0	
209.0457	$C_{10}H_9O_5^-$	?	S	-0.2	Biomass burning[21]
			D	-0.9	
210.9918	$C_5H_7O_7S^-$		S	-0.1	Isoprene organosulfate chemistry[1]
			D	-0.8	
			J	-0.5	
213.0074	$C_5H_9O_7S^-$		S	-0.4	Isoprene organosulfate chemistry[1]
			D	-0.3	
			J	0.9	
215.0231	$C_5H_{11}O_7S^-$		S	-0.2	Isoprene organosulfate chemistry[1]
			D	0.0	
			J	-0.5	
215.0561	$C_9H_{11}O_6^-$	?	S	0.4	Monoterpene oxidation[22]
			D	-1.3	
			J	0.1	
221.0667	$C_8H_{13}O_7^-$		S	-0.4	Isoprene oxidation[1]
			J	-0.5	
223.0282	$C_7H_{11}O_6S^-$		S	-0.1	Monoterpene organosulfate[23]
			D	-0.9	
229.0024	$C_5H_9O_8S^-$		S	0.3	Isoprene organosulfate chemistry[1]
			D	0.4	
			J	0.5	
231.0180	$C_5H_{11}O_8S^-$	?	S	-0.2	Isoprene organosulfate chemistry[15]
			D	-0.2	
			J	0.0	

Mass	Formula	Structure		Value	Source
233.0667	$C_9H_{13}O_7^-$	?	S D J	-0.8 -0.9 -0.7	Monoterpene oxidation[24,25]
235.1187	$C_{10}H_{19}O_6^-$		D J	-0.1 0.4	Isoprene oxidation, accretion product[26]
239.0231	$C_7H_{11}O_7S^-$		S D J	0.2 -0.6 0.7	Monoterpene or methacrolein organosulfate[27,28]
247.0823	$C_{10}H_{15}O_7^-$	?	S D J	0.7 -1.2 -0.5	Monoterpene oxidation[24,25]
251.0595	$C_9H_{15}O_6S^-$		S D	-0.8 -0.8	Monoterpene organosulfate[28,29]
253.0388	$C_8H_{13}O_7S^-$		S D J	-0.9 -0.8 0.0	Monoterpene or isoprene organosulfate[30,31]
253.1293	$C_{10}H_{21}O_7^-$		S J	-0.4	Isoprene oxidation, accretion product[26]
260.0082	$C_5H_{10}O_9NS^-$		D J	-0.5 0.6	Isoprene nitrooxy-organosulfate[1]
267.0544	$C_9H_{15}O_7S^-$	?	S D J	-0.3 -1.2 0.1	Monoterpene organosulfate[32]
279.0544	$C_{10}H_{15}O_7S^-$		D J	0.1 -0.2	Monoterpene organosulfate[33]
294.0653	$C_{10}H_{16}O_7NS^-$		D	-1.3	Monoterpene nitrooxy-organosulfate[28]

Mass	Formula	Structure	Sample*	Error	Marker compound
296.0446	$C_9H_{14}O_8NS^-$		D	-1.5	Monoterpene nitrooxy-organosulfate[28]
304.9933	$C_5H_9O_{11}N_2S^-$		S	-1.1	Isoprene nitrooxy-organosulfate[1]
315.0755	$C_{10}H_{19}O_9S^-$		S D J	-1.8 -0.8 -0.3	Isoprene organosulfate accretion product[26]
333.0861	$C_{10}H_{21}O_{10}S^-$		S J	0.5 -0.5	Isoprene organosulfate accretion product[26]

*S = September 2016 sample, D = December 2016 sample, J = June 2017 sample.

**Marker compound references:

1. Claeys, M. & Maenhaut, W. Secondary Organic Aerosol Formation from Isoprene: Selected Research, Historic Account and State of the Art. *Atmosphere (Basel)* **12**, (2021).
2. Kawamura, K., Sempéré, R., Imai, Y., Fujii, Y. & Hayashi, M. Water soluble dicarboxylic acids and related compounds in Antarctic aerosols. *Journal of Geophysical Research: Atmospheres* **101**, 18721–18728 (1996).
3. Nguyen, T. B. *et al.* High-resolution mass spectrometry analysis of secondary organic aerosol generated by ozonolysis of isoprene. *Atmos Environ* **44**, 1032–1042 (2010).
4. Krechmer, J. E. *et al.* Formation of Low Volatility Organic Compounds and Secondary Organic Aerosol from Isoprene Hydroxyhydroperoxide Low-NO Oxidation. *Environ Sci Technol* **49**, 10330–10339 (2015).
5. Surratt, J. D. *et al.* Evidence for Organosulfates in Secondary Organic Aerosol. *Environ Sci Technol* **41**, 517–527 (2007).
6. Rollins, A. W. *et al.* Isoprene oxidation by nitrate radical: alkyl nitrate and secondary organic aerosol yields. *Atmos Chem Phys* **9**, 6685–6703 (2009).
7. Claeys, M. *et al.* Hydroxydicarboxylic Acids: Markers for Secondary Organic Aerosol from the Photooxidation of α-Pinene. *Environ Sci Technol* **41**, 1628–1634 (2007).
8. Jaoui, M. *et al.* Organic Hydroxy Acids as Highly Oxygenated Molecular (HOM) Tracers for Aged Isoprene Aerosol. *Environ Sci Technol* **53**, (2019).
9. Jiang, H. *et al.* Formation of organic sulfur compounds through SO2-initiated photochemistry of PAHs and dimethylsulfoxide at the air-water interface. *Atmos Chem Phys* **22**, 4237–4252 (2022).
10. Samaké, A. *et al.* Arabitol, mannitol, and glucose as tracers of primary biogenic organic aerosol: the influence of environmental factors on ambient air concentrations and spatial distribution over France. *Atmos Chem Phys* **19**, 11013–11030 (2019).
11. Iinuma, Y., Böge, O., Gräfe, R. & Herrmann, H. Methyl-Nitrocatechols: Atmospheric Tracer Compounds for Biomass Burning Secondary Organic Aerosols. *Environ Sci Technol* **44**, 8453–8459 (2010).
12. Kleindienst, T. E. *et al.* Estimates of the contributions of biogenic and anthropogenic hydrocarbons to secondary organic aerosol at a southeastern US location. *Atmos Environ* **41**, 8288–8300 (2007).
13. Kenseth, C. M. *et al.* Synthesis of Carboxylic Acid and Dimer Ester Surrogates to Constrain the Abundance and Distribution of Molecular Products in α-Pinene and β-Pinene Secondary Organic Aerosol. *Environ Sci Technol* **54**, (2020).
14. Medeiros, P. M., Conte, M. H., Weber, J. C. & Simoneit, B. R. T. Sugars as source indicators of biogenic organic carbon in aerosols collected above the Howland Experimental Forest, Maine. *Atmos Environ* **40**, 1694–1705 (2006).
15. Chen, Y. *et al.* Heterogeneous Hydroxyl Radical Oxidation of Isoprene-Epoxydiol-Derived Methyltetrol Sulfates: Plausible Formation Mechanisms of Previously Unexplained Organosulfates in Ambient Fine Aerosols. *Environ Sci Technol Lett* **7**, 460–468 (2020).
16. Kahnt, A. *et al.* 2-Hydroxyterpenylic Acid: An Oxygenated Marker Compound for α-Pinene Secondary Organic Aerosol in Ambient Fine Aerosol. *Environ Sci Technol* **48**, 4901–4908 (2014).

17. Tao, S. *et al.* Molecular Characterization of Organosulfates in Organic Aerosols from Shanghai and Los Angeles Urban Areas by Nanospray-Desorption Electrospray Ionization High-Resolution Mass Spectrometry. *Environ Sci Technol* **48**, 10993–11001 (2014).
18. Szmigielski, R. *et al.* 3-methyl-1,2,3-butanetricarboxylic acid: An atmospheric tracer for terpene secondary organic aerosol. *Geophys Res Lett* **34**, L24811 (2007).
19. Molteni, U. *et al.* Formation of highly oxygenated organic molecules from aromatic compounds. *Atmos Chem Phys* **18**, 1909–1921 (2018).
20. Kong, X. *et al.* Molecular characterization and optical properties of primary emissions from a residential wood burning boiler. *Science of The Total Environment* **754**, 142143 (2021).
21. Mabato, B. R. G. *et al.* Aqueous secondary organic aerosol formation from the direct photosensitized oxidation of vanillin in the absence and presence of ammonium nitrate. *Atmos Chem Phys* **22**, 273–293 (2022).
22. Amorim, J. V. *et al.* Photo-oxidation of pinic acid in the aqueous phase: a mechanistic investigation under acidic and basic pH conditions. *Environmental Science: Atmospheres* **1**, 276–287 (2021).
23. Yassine, M. M., Dabek-Zlotorzynska, E., Harir, M. & Schmitt-Kopplin, P. Identification of Weak and Strong Organic Acids in Atmospheric Aerosols by Capillary Electrophoresis/Mass Spectrometry and Ultra-High-Resolution Fourier Transform Ion Cyclotron Resonance Mass Spectrometry. *Anal Chem* **84**, 6586–6594 (2012).
24. Jokinen, T. *et al.* Production of extremely low volatile organic compounds from biogenic emissions: Measured yields and atmospheric implications. *Proceedings of the National Academy of Sciences* **112**, 7123–7128 (2015).
25. Liu, D. *et al.* Large differences of highly oxygenated organic molecules (HOMs) and low-volatile species in secondary organic aerosols (SOAs) formed from ozonolysis of *β* -pinene and limonene. *Atmos Chem Phys* **23**, 8383–8402 (2023).
26. Armstrong, N. C. *et al.* Isoprene Epoxydiol-Derived Sulfated and Nonsulfated Oligomers Suppress Particulate Mass Loss during Oxidative Aging of Secondary Organic Aerosol. *Environ Sci Technol* **56**, 16611–16620 (2022).
27. Nozière, B., Ekström, S., Alsberg, T. & Holmström, S. Radical-initiated formation of organosulfates and surfactants in atmospheric aerosols. *Geophys Res Lett* **37**, (2010).
28. Surratt, J. D. *et al.* Organosulfate Formation in Biogenic Secondary Organic Aerosol. *J Phys Chem A* **112**, 8345–8378 (2008).
29. Wang, Y., Ren, J., Huang, X. H. H., Tong, R. & Yu, J. Z. Synthesis of Four Monoterpene-Derived Organosulfates and Their Quantification in Atmospheric Aerosol Samples. *Environ Sci Technol* **51**, 6791–6801 (2017).
30. Schindelka, J., Iinuma, Y., Hoffmann, D. & Herrmann, H. Sulfate radical-initiated formation of isoprene-derived organosulfates in atmospheric aerosols. *Faraday Discuss* **165**, 237 (2013).
31. Yang, T. *et al.* Spatial and diurnal variations of aerosol organosulfates in summertime Shanghai, China: potential influence of photochemical processes and anthropogenic sulfate pollution. *Atmos Chem Phys* **23**, 13433–13450 (2023).
32. Ye, J., Abbatt, J. P. D. & Chan, A. W. H. Novel pathway of SO2 oxidation in the atmosphere: reactions with monoterpene ozonolysis intermediates and secondary organic aerosol. *Atmos Chem Phys* **18**, 5549–5565 (2018).
33. Xu, R. *et al.* Chemical transformation of a-pinene-derived organosulfate via heterogeneous OH oxidation: implications for sources and environmental fates of atmospheric organosulfates. *Atmos Chem Phys* **22**, 5685–5700 (2022).

Table S2. 24-h averaged meteorology data obtained from ERA5 reanalysis for the three seasonal periods studied: 10 - 30 September 2016 (SEP), 18 November - 23 December 2016 (DEC), and 22 May - 21 June 2017 (JUN). Data was averaged from one grid cell located at the measurement site (lat, lon) (-2.9°, -55°). Range of hourly data shown in parentheses.

Meteorological Variable	JUN	SEP	DEC
Surface Temperature (°C) (Min – Max)	27.1 (23.9 – 32.0)	28.0 (23.9 – 32.8)	27.7 (23.6 – 33.0)
Relative Humidity (%)	82.5 (56.6 – 94.0)	77.7 (53.4 – 94.0)	79.1 (50.4 – 94.7)
Precipitation (mm)*	0.16 (0 -3.5)	0.23 (0 – 3.9)	0.50 (0 – 9.0)
Daytime solar radiation at surface (kJ/m^2)**	155 (0.64 – 370)	188 (1.7 – 436)	174 (0.74 – 431)
Total Cloud Cover (%)	51.9 (0.0-100)	67.7 (0.0-100)	82.4 (0.0-100)
Boundary Layer Height (m)	431 (68.6 – 1249)	495 (56.8 – 1261)	482 (30.1 – 1470)
Cloud Base Height (m)	983 (32.1 – 8437)	1409 (121-10400)	1357 (168 – 14420)
Total Column Water (kg/m^2)	49.2 (36.4 – 61.6)	47.3 (35.5-57.9)	52.3 (35.7 – 70.4)
Leaf Area Index (m^2/m^2)	3.2 (2.9 – 3.4)	3.3 (3.2 – 3.3)	2.7 (2.6 – 2.9)

*Defined as the total condensed water that reaches Earth's surface accumulated over a 1 h period.
**Average obtained after removing times of no solar radiation (nighttime).